

# Rational Design of Cholesterol Derivative for Improved Stability of Paclitaxel Cationic Liposomes

Jasmin Monpara<sup>1</sup> · Chryso Kanthou<sup>2</sup> · Gillian M. Tozer<sup>2</sup> · Pradeep R. Vavia<sup>1</sup>

Received: 14 September 2017 / Accepted: 10 February 2018

© Springer Science+Business Media, LLC, part of Springer Nature 2018

## ABSTRACT

**Purpose** This work explores synthesis of novel cholesterol derivative for the preparation of cationic liposomes and its interaction with Paclitaxel (PTX) within liposome membrane using molecular dynamic (MD) simulation and in-vitro studies.

**Methods** Cholesteryl Arginine Ethylester (CAE) was synthesized and characterized. Cationic liposomes were prepared using Soy PC (SPC) at a molar ratio of 77.5:15:7.5 of SPC/CAE/PTX. Conventional liposomes were composed of SPC/cholesterol/PTX (92:5:3 M ratio). The interaction between paclitaxel, ligand and the membrane was studied using 10 ns MD simulation. The interactions were studied using Differential Scanning Calorimetry (DSC) and Small Angle Neutron Scattering analysis. The efficacy of liposomes was evaluated by MTT assay and endothelial cell migration assay on different cell lines. The safety of the ligand was determined using the Comet Assay.

**Results** The cationic liposomes improved loading efficiency and stability compared to conventional liposomes. The increased PTX loading could be attributed to the hydrogen bond between CAE and PTX and deeper penetration of PTX in the bilayer. The DSC study suggested that inclusion of CAE in the DPPC bilayer eliminates  $T_g$ . SANS data

showed that CAE has more pronounced membrane thickening effect as compared to cholesterol. The cationic liposomes showed slightly improved cytotoxicity in three different cell lines and improved endothelial cell migration inhibition compared to conventional liposomes. Furthermore, the COMET assay showed that CAE alone does not show any genotoxicity. **Conclusions** The novel cationic ligand (CAE) retains paclitaxel within the phospholipid bilayer and helps in improved drug loading and physical stability.

**KEY WORDS** COMET assay · molecular dynamic simulation · paclitaxel-loaded cationic liposomes · trans-well migration assay

## ABBREVIATIONS

<sup>1</sup> HNMR	Proton nuclear magnetic resonance
CAE	Cholesteryl arginine ethylester
DMEM	Dulbecco's modified eagle's medium
DPX	Disterene plasticizer xylene
H5V	Mouse endothelial cell line
HDMEC	Human dermal microvascular endothelial cells
IC50	Concentration at which 50% inhibition seen
IntraHB	Intramolecular hydrogen bonds
LMP	Low melting point
MD Simulation	Molecular dynamic simulation
MDA-MB 231	Human breast cancer adenocarcinoma cell line
MolSA	Molecular surface area
MTT	3-(4,5-dimethylthiazol-2yl)-2,5-diphenyltetrazolium bromide
OD	Optical density
OPLS3	Optimized potentials for liquid simulations
POPC	1-palmitoyl-2-oleoyl-sn-glycero-3-phosphocholine

**Electronic supplementary material** The online version of this article (<https://doi.org/10.1007/s11095-018-2367-8>) contains supplementary material, which is available to authorized users.

✉ Pradeep R. Vavia  
pr.vavia@ictmumbai.edu.in

<sup>1</sup> Department of Pharmaceutical Sciences and Technology, University under Section 3 of UGC Act – 1956, Elite Status and Center of Excellence – Govt. of Maharashtra, TEQIP Phase II Funded, Institute of Chemical Technology Mumbai 400019, India

<sup>2</sup> Tumor Microcirculation Group, Department of Oncology & Metabolism School of Medicine, The University of Sheffield Sheffield, UK

PSA	Polar surface area
PTX	Paclitaxel
RMSD	Relative mean square deviation
SASA	Solvent accessible surface area
SPC	Soy phosphatidylcholine
TIP3P	Transferable intermolecular potential with 3 points
TLC	Thin layer chromatography

## INTRODUCTION

Paclitaxel (PTX) is one of the most widely used anticancer drugs (1). It was first approved as Taxol® for use in ovarian, lung and breast cancer, as well as AIDS-related Kaposi's sarcoma. Taxol® is formulated in a (50:50 *v/v*) mixture of Cremophor® EL (polyethoxylated castor oil) and dehydrated alcohol and given as an infusion of a diluted 0.3–1.2 mg/ml solution in 0.9% sodium chloride or similar, over one to three hours (2). However, there are several drawbacks to this formulation, which include development of severe hypersensitivity reaction to Cremophor® EL and alcohol-induced phlebitis at the injection site (3). Microprecipitation of PTX in the infusion vehicle and leaching of plasticizers from the infusion can also occur. An alternative PTX formulation, free of Cremophor® EL, was approved by the FDA in 2005 as Abraxane® for the treatment of metastatic breast cancer (4). Abraxane® is a freeze dried formulation of albumin-bound PTX, which upon reconstitution produces nanoparticles of 130 nm diameter average size (5). Although Abraxane® is associated with improved tumor response, it has poor colloidal stability in the blood circulation, resulting in release of free PTX into the bloodstream from disassembly of the Abraxane® nanoparticles (6).

There are numerous reports advocating liposomes as an alternative to Taxol® for improved PTX delivery to tumours (7). For instance, liposomes can alter the pharmacokinetics and distribution profile of PTX favoring improved clinical outcomes (8). Currently, there are several liposomal PTX formulations in development, but Lipusu® is the only one approved so far (9). In addition, LEP-ETU® developed by NeoPharm (10) has completed Phase II clinical studies and EndoTag-1® developed by Medigene AG (11) has also completed Phase II clinical studies, as a tumor endothelial cell targeted PTX delivery system. Cationic liposome based targeting of an anti-angiogenic agent to tumor endothelial cells has gained tremendous attention in the last decade due to preferential distribution to angiogenic blood vessels (12). Hiroshi Kiwada *et al.* has reviewed the cationic liposomes for targeting anticancer drug to the tumor vasculature, their in-vivo pharmacokinetics and toxicity and their clinical applications (13). The mechanism by which this distribution occurs is still unclear, although it is commonly believed to relate to an electrostatic interaction between the positive charge of

cationic liposomes and the negatively charged glycocalyx of endothelial cells (14). PTX is a suitable drug for vascular targeted delivery systems as, apart from its use as first-line chemotherapy in several cancers, it also has anti-angiogenic properties (15). Metronomic doses of PTX have been shown to downregulate vascular endothelial growth factor (VEGF) and angiopoietin-1, and inhibit several endothelial cell functions in-vitro such as proliferation, migration, metalloprotease production and morphogenesis (16). Despite the potential advantages of liposomal PTX, its development has witnessed slow progress mainly due to instability of PTX within the liposomal bilayer (17). Therefore, pharmaceutical development is still required to develop a PTX formulation with higher loading efficiency and sufficient colloidal stability (18).

Molecular dynamic (MD) simulation is a force-field based simulation that is used to calculate the behavior of a molecule in given surroundings, taking into account the molecular motions such as vibration, bond stretching, angle bendings, and bond formation (19). MD simulation is a tool to simulate the interactions of drugs and proteins with the cellular membrane. MD simulation is being increasingly used to study the interactions of drugs within liposome membrane because of the close resemblance of liposomes with cellular membranes (20). For instance, Stepniewski *et al.* studied the surface structure of PEGylated liposomes and its interaction with an ionic environment (21). Kang and Loverde studied the molecular interaction of hydrophobic drugs with a phospholipid bilayer (22). Jämbeck *et al.* reported MD studies of liposomes as a carrier for hypericin using coarse grain models (23).

In the present study, we have designed and evaluated an arginine conjugated cholesterol derivative; cholesteryl arginine ethyl ester (CAE) in cell-free and cell systems. Arginine is considered the most hydrophilic of the natural amino-acids. The guanidinium group of arginine has the capacity for up to six hydrogen bonds (H-bonds). The resonance stabilized group has pKa over 12, and thus arginine is protonated and positively charged in all biological conditions (24). Cholesterol, due to its effect on membrane fluidity, provides stability to the liposome bilayer. Additionally, metabolism of CAE should follow normal biological metabolic pathways for cholesterol and arginine and therefore CAE can be considered biodegradable. Thus, CAE has potential as a suitable ligand to provide stability and positive charge to PTX liposomes.

## MATERIALS AND METHODS

### Materials

Unsaturated Soy phosphatidylcholine (SPC) and 1,2-dipalmitoyl-sn-glycero-3-phosphocholine (DPPC) were obtained from Lipoid GmbH (Ludwigshafen, Germany). Cholesteryl Arginine Ethyl Ester (CAE) was synthesized and purified in-

house following established procedures (25,26). PTX was obtained from Dr. Reddy's laboratories Ltd. (Hyderabad, India). Cholesterol was purchased from Merck India Pvt. Ltd. (Mumbai, India). 3-(4,5-dimethylthiazol-2-yl)-2,5-diphenyltetrazolium bromide (MTT) was purchased from Sigma-Aldrich Co Ltd. (Dorset, UK). Comet Assay kit was purchased from Trivigen Inc. (AMS Biotechnology (Europe) Limited, Abingdon, UK). All other reagents were of analytical grade and purchased from Merck India Pvt. Ltd. (Mumbai, India).

## Cell Lines

The immortalised mouse Endothelial Cell line H5V was a kind gift from Dr. Annunciata Vecchi (27). The human breast cancer adenocarcinoma cell line (MDA-MB 231) was from ATCC (ATCC HTB-26). Both H5V and MDA MB 231 cells were maintained in Dulbecco's modified Eagle's medium (DMEM, Lonza, UK) supplemented with 10% heat-inactivated FBS, 10 mM L-glutamine, 100 U/ml penicillin and 100 µg/ml streptomycin in a 5% CO<sub>2</sub> /air incubator at 37°C. Human Dermal Microvascular Endothelial Cells (HDMEC) were purchased from PromoCell GmbH and maintained in Endothelial Cell Growth Medium MV2 (PromoCell GmbH) supplemented with Supplement Mix C-39226 (PromoCell GmbH), 100 U/ml penicillin and 100 µg/ml streptomycin in a 5% CO<sub>2</sub> /air incubator at 37°C.

## Computational Methods

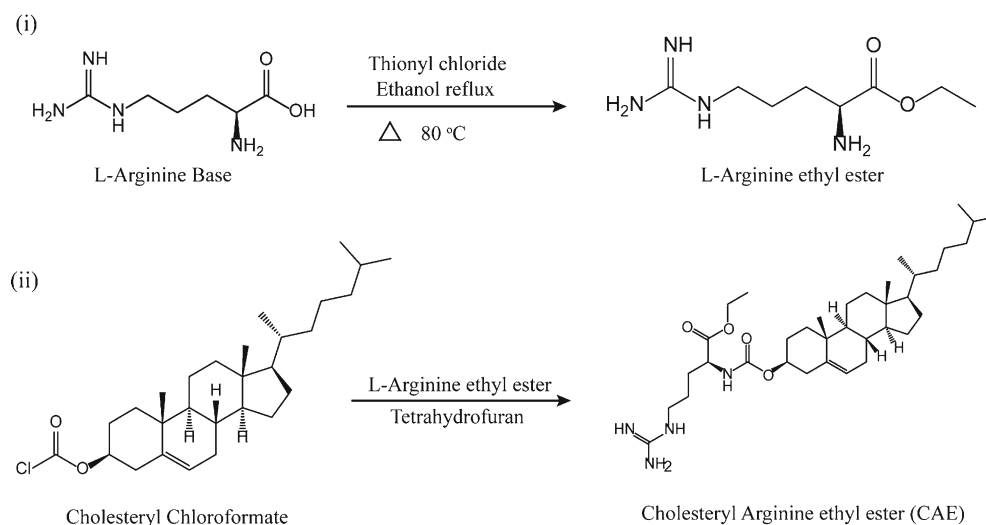
The structures of PTX, CAE, Arginine ethyl ester (AEE), and Cholesterol for initial studies were generated using ChemBioOffice® V.16 and saved as structure-data files (.sdf). Structures were imported into Maestro® 10.2 module of Schrödinger® Discovery Suite Release 2016–2. LigPrep® module was used to generate 3D structures of possible

tautomers, isomers or ionization states from flat the geometry of .sdf file using Epik followed by geometry optimization based on the OPLS3 force field. pKa prediction of CAE was performed using empirical Epik® workflow. Other chemical parameters were calculated using QikProp®. Further calculations were carried out using MacroModel® module and the OPLS3 force field as implemented in MacroModel®. The energy of the PTX and CAE was minimized using MacroModel-minimization step. Pre-equilibration of lipid bilayer composed of 1-palmitoyl-2-oleoyl-sn-glycero-3-phosphocholine (POPC) phospholipid and embedding PTX and CAE or PTX and Cholesterol was performed using the Desmond® program. The predefined transferable intermolecular potential functions (TIP3P) water model was used to assimilate water molecules. Appropriate Na<sup>+</sup> and Cl<sup>-</sup> were added to neutralize the systems. The total number of atoms in the investigated systems was approximately 10, 430 including about 2000 water molecules and 40 POPC phospholipids. The orthorhombic periodic box dimensions were set to 10 Å X 10 Å X 10 Å. After building the solvated system, minimization and relaxation of the membrane were performed using the OPLS3 force field in Desmond®. MD simulation was performed using Desmond® at constant temperature and pressure (NPT ensemble; 300 K, 1.01325 bars) for 10 ns.

## Synthesis of Cholesteryl Arginine Ethyl Ester

The designed Cholesteryl Arginine Ethyl Ester was synthesized by esterification of L-arginine with ethanol to form L-Arginine ethyl ester 2HCl (AEE) followed by N-amidation using Cholesteryl chloroformate to form the final product, Cholesteryl Arginine Ethyl Ester (CAE), as shown in Fig. 1. Briefly, L-Arginine (base) (2 g) was dispersed in ethanol (100 ml) in a round bottom flask and cooled to 10°C. Thionyl chloride (1.5 Mole equivalents; 1.2 ml) was added

**Fig. 1** Schematics for the synthesis of Cholesteryl arginine ethyl ester.



dropwise to the mixture. The mixture was refluxed for 4 h at 60°C to carry out esterification. The reaction was monitored by TLC using Butanol-Acetic Acid-Water (3:1:1) as mobile phase and ninhydrin solution for detection of the product. After completion of the reaction, excess ethanol was removed by vacuum drying to obtain a yellowish liquid, AEE. AEE was solubilized into 50 ml Tetrahydrofuran: water (50:50) mixture and pH was adjusted to 9.0 with 1 M NaOH solution. Further, amidation was carried out by Schotten-Baumann reaction using Cholesteryl chloroformate (25). Cholesteryl chloroformate (0.9 Mole equivalent; 4.6 g) was solubilized in 30 ml Tetrahydrofuran and added drop-wise to L-Arginine Ethyl Ester solution under continuous stirring with pH of the reaction mixture was maintained between 7.5–7.8. The whole reaction was carried out at 10–15°C for 6–7 h. The reaction was monitored by TLC as mentioned above. After completion of the reaction, pH was neutralized by adding dilute HCl solution. Tetrahydrofuran was removed by vacuum evaporation. The final product was extracted with chloroform and dried using rotary evaporator. The product was eluted with CH<sub>2</sub>Cl<sub>2</sub>/CH<sub>3</sub>OH (9:1 v/v) from a silica gel (70–230 mesh), and the solvent was removed under reduced pressure to give a light yellowish solid (5.0 g, 70% yield), R<sub>f</sub> = 0.6 (CH<sub>2</sub>Cl<sub>2</sub>/CH<sub>3</sub>OH 4:1 V/V). The elute were analyzed using Anisaldehyde as a developer in TLC to confirm cholesterol backbone. The <sup>1</sup>H NMR spectrum was recorded using a Bruker® 800 MHz spectrophotometer using spectroscopic grade CDCl<sub>3</sub>. Molecular mass determination of the synthesized compounds was carried out using LC-MS (Finnigan LCQ Advantage Max, Thermo electron corporation, USA). Anal. Calcd. for C<sub>36</sub>H<sub>62</sub>N<sub>4</sub>O<sub>4</sub> (MW 614.92): C, 70.32; H, 10.16; N, 9.11; O, 10.41. Found: C, 70.20; H, 10.20; N, 9.30; O, 10.30. MS (positive/negative ES): m/z 615.27 [M + H]<sup>+</sup>, <sup>1</sup>H NMR (800 MHz, CDCl<sub>3</sub>, 20°C, TMS) 0.854–0.868 (6H, m, 1), 0.9–3 (aliphatic protons of cholesteryl and arginine moiety, 40H, m, unlabelled), 4.189–4.211 (2H, triplet, f), 4.43 (1H, s, e), 5.32 (1H, s, d), 5.829–5.837 (1H, doublet, c), 6.972 (4H, broad s, b), 7.71 (1H, broad s, a).

### Preparation of Liposomes

The liposomes were prepared by the thin film hydration method. Briefly, lipids and PTX were dissolved in 3 ml of chloroform. The thin film was prepared using a 250-ml round bottom flask and vacuum evaporator at 60°C under reduced pressure. The film was hydrated using 0.9% w/v NaCl solution at 60°C. Cationic liposomes were composed of SPC/CAE/PTX (77.5:15:7.5 M ratio). The conventional liposomes were composed of SPC/cholesterol/PTX (92: 5: 3 M ratio). For the preparation of blank cationic liposomes and blank conventional liposomes, PTX was omitted from the formulation. The total solid content of the liposomal dispersion was kept constant to 10 mM/10 ml in each case. The suspension of

large multilamellar liposomes was extruded through a polycarbonate membrane of pore size 200 nm using lipid extruder (Lipex Biomembrane Inc., Canada) to form small unilamellar liposomes of uniform particle size. For Differential Scanning Calorimetry, DPPC was used instead of SPC to prepare liposomes. The particle size and zeta potential of liposomes were measured by dynamic light scattering and electrophoretic light scattering, respectively, using Malvern Zetasizer (Malvern Instrument Ltd., UK).

### Drug Loading Efficiency

PTX loading was determined using a reported method (28). Briefly, Sephadex G-25 gel was autoclaved in ultra-purified water to allow hydration of Sephadex G-25 particles. The column was formed in 5 ml syringe by placing glass wool at the bottom of the syringe and centrifuging at 350 g for 5 min. The dry column was loaded with 1 ml blank liposomes to saturate the column. The loaded column was then centrifuged at 1520 g for 5 min to remove the blank liposomes. Subsequently, PTX liposomes were added to the column and centrifuged at 1520Xg for 5 min. PTX was extracted from one ml of elute using tert-butyl methyl ether on a vortex mixer for 60 s. Upon centrifugation at 1520Xg for 10 min, the separated organic layer was then transferred to clean centrifuge tube and dried using nitrogen at 40°C. PTX content was determined using a reverse phase HPLC system (Waters, USA) unit, Hypersil C-18 column (250 × 4.6 mm, 5 μ). The mobile phase consisted of acetonitrile: water (60:40). The analysis was performed at a flow rate of 1.0 ml/min with UV detection at 227 nm (29). Loading efficiency was determined using following equation:

$$\text{Loading Efficiency} = (\text{Amount of drug in liposomes} \div \text{Amount of lipid in liposomes}) \times 100$$

### Stability of Liposomes

Stability of liposomes was observed at 2–8°C for three months. After the preparation of liposomes, 2 ml aliquots were removed from the stability samples and subjected to particle size determination, zeta potential measurement, and drug loading measurement.

### Differential Scanning Caorimetry (DSC)

For DSC study, DPPC liposomes were prepared using DPPC instead of SPC in same molar ratios as described above. Briefly, a thin film of the liposome constituents was hydrated using water at 60°C for few hours. The final lipid concentration was adjusted to 30 wt%. The mixture was resuspended using vigorous vortex mixing and subsequently using ultrasonication to yield homogenous multilamellar vesicles.

The dispersions (30 μL) were filled into DSC pans made of aluminum, hermetically sealed and were stored overnight at 4°C. DSC measurements were performed by using Perkin Elmer Pyris 6 DSC (USA) with empty aluminum pans as reference. The heating thermograms were obtained between 20°C and 55°C at a scan rate of 2°C/min. Baseline correction was performed using Pyris DSC software version 8.0.

### Small Angle Neutron Scattering (SANS)

To evaluate the effect of CAE and Cholesterol on SPC liposomes, SANS study was carried out. The study was performed using SANS instrument in DHRUVA reactor at the Bhabha Atomic Research Centre (BARC) in Trombay, India (30). The samples were poured in a 0.5 cm path-length UV grade quartz sample holder with tight-fitting Teflon® stoppers and sealed with parafilm. The mean wavelength of the monochromatized beam is 5.2 Å with a spread of Δλ/λ ~ 15%. The angular distribution of neutrons scattered by the sample is recorded using a 1 m long one-dimensional He<sup>3</sup> position sensitive detector. The instrument covers a Q-range of 0.015–0.35 Å<sup>-1</sup>. The temperature in all the measurements was kept fixed at 30°C.

Scattering intensities from the sample solutions were corrected for detector background and sensitivity, empty cell scattering, and sample transmission and solvent intensity was subtracted from that of the sample and the resulting corrected intensities were normalized to absolute cross-section units.

#### Small-Angle Neutron Scattering Analysis

The differential scattering cross-section per unit volume (dΣ/dΩ) as measured for a system of monodisperse particles in a medium can be expressed as

$$\left(\frac{d\Sigma}{d\Omega}\right)(Q) = nV^2(\rho_p - \rho_s)^2 P(Q)S(Q) + B,$$

where n denotes the number density of particles, ρ<sub>p</sub> and ρ<sub>s</sub> are, respectively, the scattering length densities of particle and solvent and V is the volume of the particle. P(Q) is the intraparticle structure factor and S(Q) is the interparticle structure factor. B is a constant term representing incoherent background, which is mainly due to the hydrogen present in the sample (31,32).

Intraparticle structure factor P(Q) is decided by the shape and size of the particle and is the square of single-particle form factor F(Q) as determined by

$$P(Q) = \langle |F(Q)|^2 \rangle$$

For a spherical particle of radius R, F(Q) is given by

$$F(Q) = 3 \left[ \frac{\sin(QR) - QR\cos(QR)}{(QR)^3} \right].$$

For a system consisting of monodisperse unilamellar vesicles (33), dΣ/dΩ can be expressed as

$$\frac{d\Sigma}{d\Omega}(Q, R) = n(\rho_v - \rho_s)^2 \left[ \frac{4}{3}\pi R^3 \frac{3J_1(QR)}{QR} - \frac{4}{3}\pi(R+t)^3 \frac{3J_1[Q(R+t)]}{Q(R+t)} \right]^2$$

where n denotes the number density of the vesicles, ρ<sub>v</sub> and ρ<sub>s</sub> are the scattering length densities of the vesicle bilayer and the solvent, respectively. R is the radius of the vesicle and t is the thickness of the bilayer. J<sub>1</sub>(x) is the first order Bessel function and is given by

$$J_1(x) = \frac{\sin x - x\cos x}{x^2}$$

The polydispersity in size distribution of particle is incorporated using the following integration

$$\frac{d\Sigma}{d\Omega}(Q) = \int \frac{d\Sigma}{d\Omega}(Q, R)f(R)dR + B,$$

where f(R) is the particle size distribution and usually accounted by a log-normal distribution as given by

$$f(R) = \frac{1}{\sqrt{2\pi}R\sigma} \exp \left[ -\frac{1}{2\sigma^2} \left( \ln \frac{R}{R_{med}} \right)^2 \right],$$

Where, R<sub>med</sub> is the median value and σ is the standard deviation (polydispersity) of the distribution. The mean radius (R<sub>m</sub>) is given by R<sub>m</sub> = R<sub>med</sub> exp.(σ<sup>2</sup>/2) (34).

The data have been analyzed by comparing the scattering from different models to the experimental data. Throughout the data analysis, corrections were made for instrumental smearing, where the calculated scattering profiles smeared by the appropriate resolution function to compare with the measured data (35). The fitted parameters in the analysis were optimized using nonlinear least-square fitting program to the model scattering (36).

### In-Vitro Cytotoxicity Study

In-vitro cytotoxicity of PTX solution (in methanol), cationic liposomes, conventional liposomes and blank liposomes devoid of PTX (all in 0.9% saline) was determined using the MTT assay. The studies were carried out on three different cell lines - MDA MB 231, H5V and HDMEC to determine the sensitivity of PTX formulations on tumour cells, immortalized mouse endothelial cells and human primary endothelial cells respectively. In separate experiments, MDA MB 231, H5V and HDMEC cells were seeded at 1\*10<sup>4</sup> cells/well,

$5 \times 10^3$  cells/well and  $2 \times 10^3$  cells/well, respectively, in 96-well flat-bottom tissue culture plates 24 h prior to assay. For MDA MB 231 and H5V, PTX solution was tested at a concentration range of 0.1 nM to 30 nM and the liposomal formulations were tested at a PTX concentration range of 10 nM to 150 nM. Because of the greater sensitivity of HDMEC to PTX, PTX solution was tested at a concentration range 0.1 nM to 10 nM and the liposomes were tested at a PTX concentration range of 0.5 nM to 30 nM for this cell type. The stock solution (1  $\mu$ M) of PTX was prepared in methanol and the stocks solutions ((1  $\mu$ M PTX) of liposomes were prepared in PBS. Further dilutions were prepared in the cell culture media for all samples. The negative control cells were incubated with the appropriate drug vehicles only.

For the MTT assay, MTT (3-(4,5-dimethylthiazol-2-yl)-2,5-diphenyl tetrazolium bromide) was dissolved in sterile PBS at a concentration of 5 mg/ml. After 72 h of incubation of cells with drugs at 37°C, as described above, 20  $\mu$ l of MTT solution was added to each well and incubated for 5 h. The unreduced MTT and medium were discarded from the wells. Then, 100  $\mu$ l of acidified isopropanol (1 ml 2 M HCl mixed with 50 ml isopropanol) was added to each well to dissolve the MTT formazan crystals. Absorbance was read at 540 nm in a microplate reader. Percentage viability was determined using the following equation:

$$\% \text{Cell Viability} = [OD(\text{Test Sample}) \div OD(\text{Untreated Control Sample})] \times 100$$

The IC<sub>50</sub> values for different PTX formulations were calculated by non-linear regression curve fitting on % cell viability vs PTX concentration plots.

### Trans-Well Cell Migration Assay

Inhibition of the migratory function of HDMEC cells by PTX solution and the PTX liposome formulation was determined using the Trans-well Migration Assay (37). Briefly,  $7.5 \times 10^4$  cells were suspended in endothelial cell medium and placed in the upper compartment of an 8- $\mu$ m pore Trans-well (Costar, Corning). After one hour, drug or liposomes were added to both the upper and lower compartments. Three different concentrations (0.1 nM, 0.5 nM and 1 nM) of PTX solution and 0.1 nM, 1 nM and 2.5 nM of PTX liposomes were tested in the assay. The cells were allowed to migrate to the lower compartment for 6 h at 37°C. After the incubation, media were removed from the Trans-wells and cells were fixed using ice-cold methanol. The cells were stained using hematoxylin solution and the cells at the proximal side of the membrane were removed using cotton swabs. The membrane was removed from the inserts and mounted to frosted slides using DPX (Distrene 80). The cells that migrated to the lower side of the membrane were counted using a microscope fitted with a 40X objective and % migration was normalized against

untreated cells. The data obtained were expressed as mean  $\pm$  standard deviation from the mean (SD) and analyzed using a one-way ANOVA within Graph Pad Prism® 7.03 statistical analysis software.  $P < 0.05$  was considered to be statistically significant. All the experiments were carried out in triplicate.

### Comet Assay

The comet assay (single cell gel electrophoresis) measures deoxyribonucleic acid (DNA) strand breaks in eukaryotic cells. Briefly, the cells are embedded in agarose gel followed by lysis by detergent and high salt concentration to form nucleoids. If the nucleoids have strand breaks, they form comet-like structures after electrophoresis at high pH that can be observed by fluorescence microscopy. The intensity of the comet tail relative to the head reflects the number of DNA breaks. The comet assay was performed to determine potential genotoxicity of the synthesized compound-CAE. CAE was dissolved in dimethyl sulphoxide (DMSO) at the level of 10 mg/ml and sufficient volume was added in the media to achieve a final concentration of 5  $\mu$ g/ml, which corresponds to the amount needed to deliver 175 mg/m<sup>2</sup> dose of PTX. A ten times higher concentration of CAE (i.e. 50  $\mu$ g/ml) was also tested to confirm the safety of the compound. The final concentration of DMSO achieved in each well was below 1% v/v which is considered non-harmful to the cells (38). Nonetheless, control cells were treated with an equivalent concentration of DMSO to nullify the effect, if any.

Briefly, in two independent experiments, HDMEC and MDA MB 231 cells were seeded into six-well plates at a density of  $5 \times 10^4$  cells/well and allowed to grow for 24 h. The test solutions were added to achieve the desired concentrations and incubated for a further 24 h. Cells treated with 200  $\mu$ M hydrogen peroxide for 20 min served as a positive control. The negative control cells were treated with an equivalent volume of DMSO mixed with media. After the incubation, cells were trypsinized and washed with PBS. Cell density was adjusted to  $1 \times 10^4$  cells/ml in PBS. The comet assay was performed using a Comet assay kit (Trivigen Inc.). The cells were suspended in LMP agarose at 37°C and allowed to set on the comet slides at room temperature. Once the cell suspension set on the slide, cell lysis was performed using the lysis buffer included in the kit for one hour at 4°C. Cell lysis was followed by DNA unwinding using alkaline unwinding solution for one hour at 4°C. After unwinding, electrophoresis was carried out at 21 V, 300mAmp for 30 min. The agarose matrix was washed twice with ultrapure water followed by 70% V/V ethanol for five minutes each and allowed to dry. The DNA was stained using SYBR® Gold dye and images were captured using fluorescence microscopy. Images were analyzed using Comet Score IV software (39). Tail moment and Olive moment were used to determine the extent of DNA damage. Each parameter gives a value comparing the amount of

DNA in the tail compared to the amount of DNA in the head calculated using fluorescence intensity. The Olive moment is used to take account of inter-sample variability. The tail moment and Olive moment were calculated as follows:

$$\text{Tail Moment} = (\text{Tail Length}) \times (\% \text{DNA in the tail})$$

$$\text{Olive Moment} = (\text{Centre of mass of tail} - \text{Centre of mass of head}) \times (\% \text{DNA in tail})$$

The data obtained was expressed as mean  $\pm$  standard deviation from the mean (SD). The data was analyzed using a one-way ANOVA within Graph Pads Prism® 7.03 statistical analysis software.  $P < 0.05$  was considered to be statistically significant.

## RESULTS AND DISCUSSION

### Chemical Parameters

The chemical parameters predicted using QikProp® are listed in Table I. The H-bond acceptor in PTX outnumbers H-bond donors. Thus, we can expect H-bond interactions of PTX with water through oxygen atoms and with CAE through guanidine nitrogen atoms (40). Generally, H-bonds of a molecule with water results in an increase in its aqueous solubility. However, the hydrogen bond interaction of PTX with water is very weak and insufficient to solubilize the molecule due to the phenomenon called “hydrophobic clustering” and higher lipophilicity ( $\log p = 4.9$ ) of PTX. Altogether, these characteristics lead to precipitation of PTX in an aqueous environment (41). CAE has a higher probability of forming H-bonds compared to cholesterol due to the presence of guanidine groups. We reasoned that this would result in a greater interaction of CAE with PTX and higher stability of PTX within the liposome bilayer.

The hydrophilic and hydrophobic surface areas (SA) provide information regarding structural features responsible for hydrophilic and hydrophobic intermolecular interactions (42). The higher hydrophobic SA of CAE and cholesterol compared to their hydrophilic SA indicates that CAE and cholesterol may have higher interaction with the lipophilic tails rather than the hydrophilic head group of the phospholipid bilayer. The pKa prediction of CAE revealed that the guanidine group of CAE has pKa more than 11 and hence is expected to be positively charged in all biological conditions.

### Atomistic Molecular Dynamic Simulation

In our study, MD simulation followed by trajectory analysis showed H-bond interaction between the guanidine group of CAE and the carbonyl group of the taxane ring of PTX, as seen in Figs. 2a1 and 3a. There was no H-bond interaction between PTX and cholesterol, rather PTX has a higher affinity towards the aqueous compartment mainly due to hydrogen bonding of carbonyl and hydroxyl groups of PTX with water molecules as shown in Figs. 2b1 and 3a. The interactions between PTX and water were not observed when cholesterol was replaced by CAE in the membrane. As shown in Fig. 2a2, b2, the MD simulation of two systems (i.e. PTX + CAE in POPC membrane and PTX + Cholesterol in POPC membrane), the sterol ring of CAE was primarily centered in the lipid bilayer core. However, the sterol ring of cholesterol centered towards the outer part of the phospholipid membrane. Apart from that, PTX was found in the vicinity of the sterol ring system of either CAE or cholesterol in both the simulations. The interaction of PTX with CAE could be explained by a higher probability of H-bond between PTX and CAE. Although H-bond was not seen between PTX and cholesterol, there might be other hydrophobic interactions strong enough to bring the taxane ring of PTX near the cholesterol molecule.

The relative mean square deviation (RMSD) plot gives a deviation of the ligand with respect to the reference conformation (0 ns). The RMSD plots of ligands (PTX: CAE or PTX: Cholesterol) (Figs. 3b and 4) show only a small change (about 2 Å) in both the simulations. Though the change in RMSD is very small, there is a noticeable difference between both the simulations. The PTX-CAE system showed higher mobility in the bilayer evident from RMSD plot referenced to time 0 ns but stabilized at 1.3 Å. The PTX-cholesterol system showed slightly lower mobility but stabilized at 1.95 Å. The Intramolecular Hydrogen Bonds (IntraHB) plot shows that PTX could frequently form two H-bonds during the simulation i.e. one intramolecular H-bond and one H-bond with CAE. However, only one intramolecular H-bond was formed in the PTX-Cholesterol system (Fig. 3a and 4). The Molecular Surface Area (MolSA) is equivalent to the van der Waals surface area. The MolSA for PTX was increased from 675 Å<sup>2</sup> to 690 Å<sup>2</sup> for in PTX: CAE liposomes but decreased from 680 Å<sup>2</sup> to 660 Å<sup>2</sup> in PTX: cholesterol liposome, which indicates an increase in van der Waals interaction between PTX

**Table I** Chemical Parameters for PTX, CAE, Cholesterol, and AEE Calculated Using QikProp®

Molecule	Mol.wt.	Volume	Total SA	Hydrophilic SA	Hydrophobic SA	H-bond donor	H-bond acceptor	log p
PTX	853.9	2271.2	1046.7	215.8	350.0	3.0	17.6	4.983
CAE	620.9	2136.0	1141.1	202.0	939.0	7.0	9.4	4.541
AEE	202.2	794.3	507.6	245.7	261.9	6	5	-0.915
Cholesterol	386.6	1390.0	736.6	49.1	658.0	1	1.7	7.03

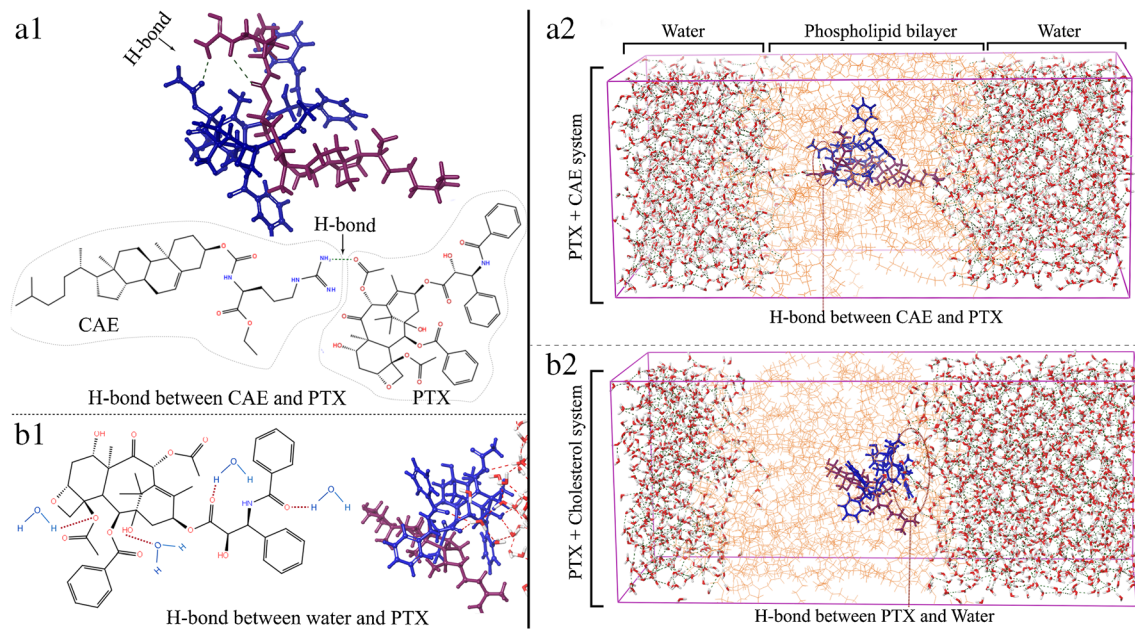


**Fig. 2** (a1)-(b1) Representation of H-bond interaction within the lipid bilayer. (a2)-(b2) Trajectories of PTX at the end of 10 ns MD simulation of (a2) PTX + CAE system and (b2) PTX + Cholesterol system. The PTX molecule is represented in blue color. CAE molecule is represented in maroon color. The simulation box is represented in pink color. The water molecule is represented in tube model and the phospholipids are represented in wire model. H-bonds are represented as green and red dashed lines. (a1)-(a2) The H-bond interaction between CAE and PTX in cationic liposomes (b1)-(b2) in conventional liposomes, Cholesterol could not form H-bonds with PTX. Moreover, due to cholesterol, the membrane showed higher water permeability and thus, water molecules could form H-bonds with PTX.

with CAE and surrounding phospholipid molecules compared to PTX-cholesterol interaction. Comparable results were found with respect to Solvent Accessible Surface Area (SASA), which indicates an increase in solvent accessible surface area (phospholipid accessible surface area in this case) in PTX-CAE system compared to decrease in SASA in PTX-Cholesterol system. This might be an additional factor resulting in higher PTX stability in bilayer when CAE is incorporated in the bilayer. The Polar Surface Area (PSA), which is the solvent accessible surface area in the molecule, contributes only by oxygen and nitrogen atoms, which remained approximately the same for both systems. Additionally, in the PTX-Cholesterol system, the membrane has higher water permeability and PTX could form H-bonds with water molecules (Fig. 2b1, b2). Kang *et al.* has reported MD simulation PTX incorporated in POPC membrane. They observed higher water penetration in the membrane and 'water fingers' in the proximity of PTX aggregates when the PTX concentration is higher than 12 mol% (22). Previous studies by Balasubramanian *et al.* and Belsito *et al.* reported that the preferential site of PTX deposition is the surface of phospholipid vesicles (43,44). The PTX molecule cannot force lipid molecules away for inserting in the bilayer and has limited access to the hydrophobic core of the bilayer (43). The self-aggregation of PTX in cholesterol containing liposomes can be explained by higher water permeability of membrane and H-bonds between PTX and water. This may in-turn expel the PTX from lipid bilayer resulting in self-aggregation

due to hydrophobicity overcoming H-bonds. The results of MD simulation indicated that CAE could be a suitable cationic ligand to prepare PTX loaded cationic liposomes.

### Formulation Development

Despite offering several advantages over conventional chemotherapy and other nano delivery systems of PTX, liposomal PTX has witnessed slow development mainly due to limitations on PTX loading and stability in the lipid bilayer (17). Several studies indicate that PTX is extremely unstable within the bilayer and self-aggregates at concentration  $\geq 3$  mol%. Previous studies of the interactions of PTX with a phospholipid bilayer suggested that, at concentrations less than 3 mol%, PTX favors the fluid state of the membrane (i.e. lowering  $T_m$ ) mainly by interaction with the surface of the phospholipid vesicle. However, at higher concentration, PTX penetration in the membrane is less due to bulkiness of the molecule and limited access to the hydrophobic region of the membrane (43). Cholesterol has been used traditionally to stabilize the lipid bilayer due to its effects on bilayer fluidity and rigidity mainly through the elimination of phase transition and decreasing membrane permeability at higher concentration. However, at low cholesterol concentration, the membrane has higher permeability due to increased membrane fluidity (45). In the presence of cholesterol, a phospholipid membrane has poor ability to incorporate PTX due to competition between the two for loading pockets in the lipid bilayer (46).

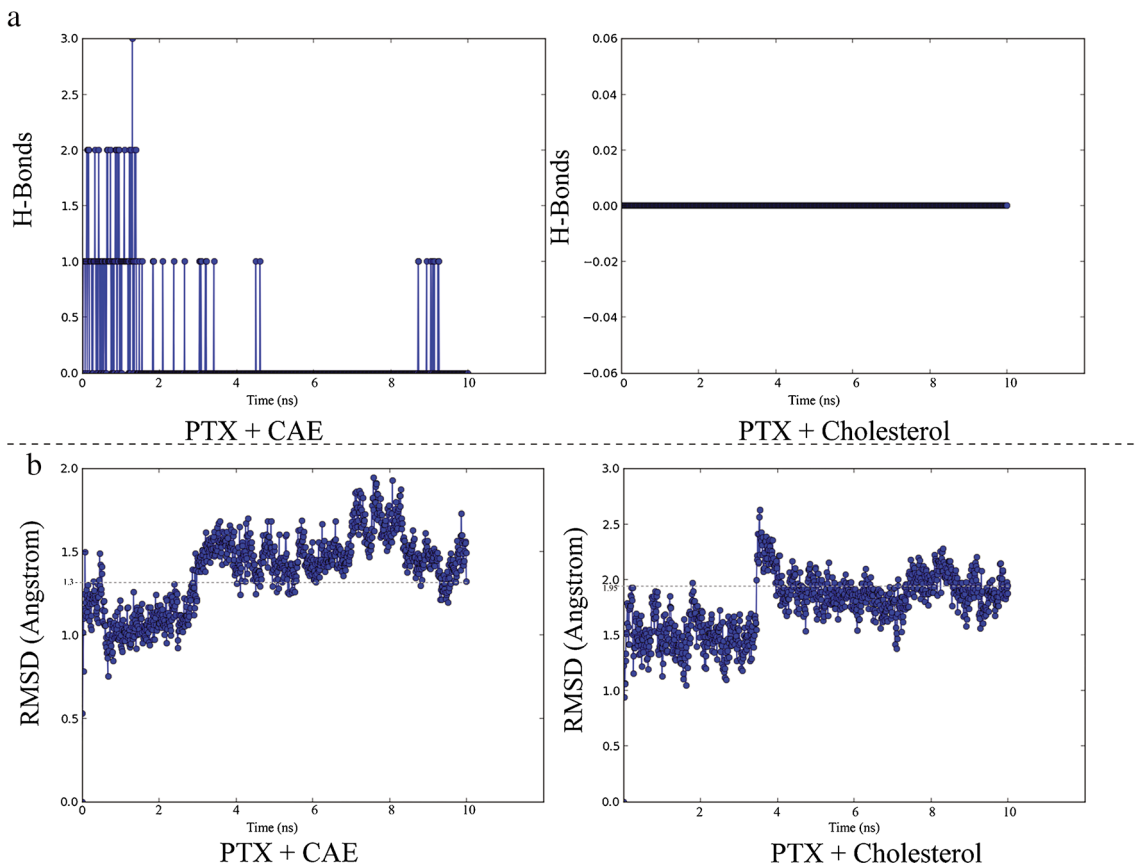


**Fig. 3** (a) H-bond plot for the MD simulation of cationic liposomes having PTX: CAE and conventional liposomes having PTX: Cholesterol. There is a H-bond interaction between PTX and CAE but no H-bonds were observed between PTX and cholesterol (b) RMSD plot for the MD simulation of cationic liposomes having PTX: CAE and conventional liposomes having PTX: Cholesterol. The ligands had slightly higher mobility in the bilayer in cationic liposome membrane.

As shown in Fig. 5a, increasing cholesterol concentration results in a decrease in PTX loading in an SPC bilayer. J. Allen Zhang *et al.* also observed a similar effect of cholesterol in a phospholipid bilayer (28). In contrast, increasing CAE concentration in the lipid bilayer did not reduce PTX loading

up to 15 mol%. Further increase in CAE concentration reduced PTX loading in the lipid bilayer. This may be attributed to a reduced number of phospholipid molecules to form an ordered bilayer which can incorporate PTX and CAE at the same time. The cationic liposomes were composed of SPC/

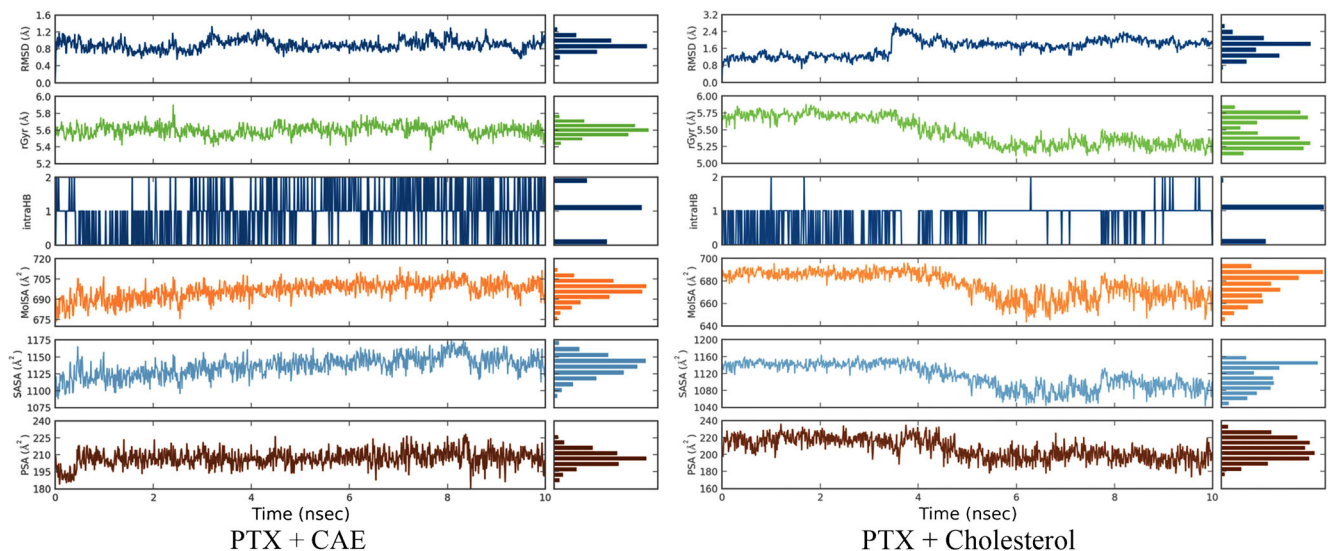


**Fig. 4** Simulation interaction diagrams both simulations (PTX: CAE system and PTX: Cholesterol system).

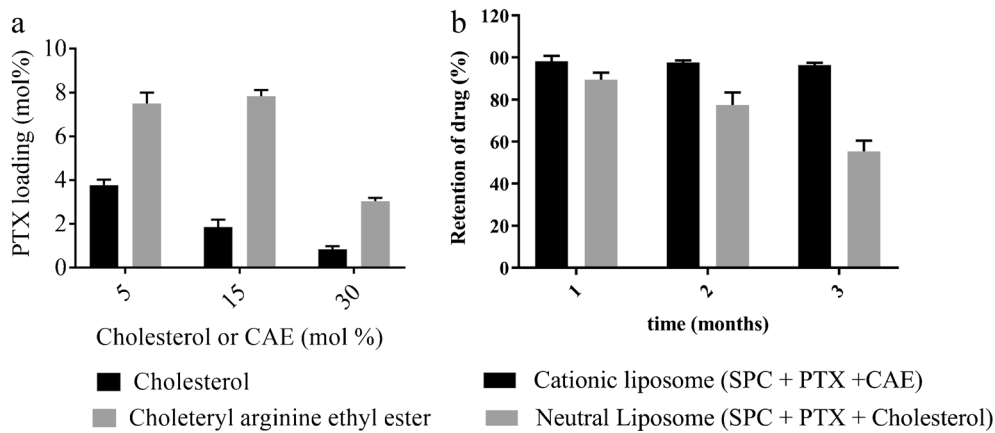


**Fig. 5** (a) PTX loading in liposome bilayer. As the concentration of cholesterol increases in the lipid bilayer, the loading of PTX decreases. However, CAE showed stabilizing effect and PTX loading did not decrease up to 15 mol%. The error bars represent the mean  $\pm$  SD of each value ( $n = 3$ ) (b) stability of liposomes over three months. The cationic liposomes retained the loaded PTX while stored at 2–8°C for three months. However, conventional liposomes showed a consistent decrease in PTX loading. The error bars represent the mean  $\pm$  SD of each value ( $n = 3$ ).

CAE/PTX (77.5:15:7.5 M ratio) with particle size  $135.4 \pm 1.3$  nm and PTX loading 7.5 mol%. The cationic liposomes had a surface charge of +40 mV. The conventional liposomes were composed of SPC/Cholesterol/PTX (92: 5: 3 M ratio) with particle size  $145.4 \pm 1.4$  nm and  $-11.7$  mV surface charge with 3 mol% PTX loading. Figure 5b shows stability testing over three months for cationic liposomes and conventional liposomes at 2–8°C. Cationic liposomes could retain PTX for the study period (approximately 98% at the end of three months). However, conventional liposomes could not retain PTX in the lipid bilayer (approximately 55% at the end of three months). The possible explanation for higher PTX loading in the presence of CAE could be deeper penetration of CAE into the hydrophobic core of the membrane. This may result in greater interaction between PTX and hydrophobic acyl chains mainly due to van der Waals interactions (22).

The results of MD simulation are in good agreement with these observations and with current research work. The MD simulation shows that in presence of cholesterol (1) PTX is primarily located at the outer hydrophobic core of the liposome (2) there is increased water permeability of the bilayer (3) increased probability of H-bond between PTX and water. These factors could be responsible for the expulsion of PTX from the bilayer, with the use of cholesterol. On the other hand, in the presence of CAE, greater PTX loading and stability might be resulting from (1) H-bond between PTX and CAE (2) deeper penetration of PTX to the hydrophobic core of the membrane and (3) decreased probability of interaction with water as shown in the MD simulation.

### Differential Scanning Calorimetry

Differential Scanning Calorimetry is most frequently used technique to determine the drug- biomembrane interactions within the formed liposomal membrane. Several

characteristic parameters can be used to describe the changes in the lipid membrane such as pretransition ( $T_p$ ), main transition ( $T_g$ ), width of transition at half peak height ( $\Delta T_{1/2}$ ) and the changes of enthalpy ( $\Delta H$ ). Upon addition of thermal energy, the pretransition  $T_p$  ( $L_\beta$  to  $P_\beta$ ) occurs between gel phase rippled phase and the main transition ( $T_m$ ) of phospholipids bilayer occurs between gel (ordered) to fluid (disordered) lamella state ( $P_\beta$  to  $L_\alpha$ ) affecting the van der waals interactions between hydrocarbon chains, increasing their mobility. The interaction of the drug molecule within the bilayer can be determined by the co-operativity of the molecules during the transition process (47).

The natural lecithins such as Egg PC and Soya PC have unsaturation in the fatty acid chains therefore, the  $T_g$  of liposomes consisting such lipids is extremely low ( $-5^\circ\text{C}$  to  $-15^\circ\text{C}$

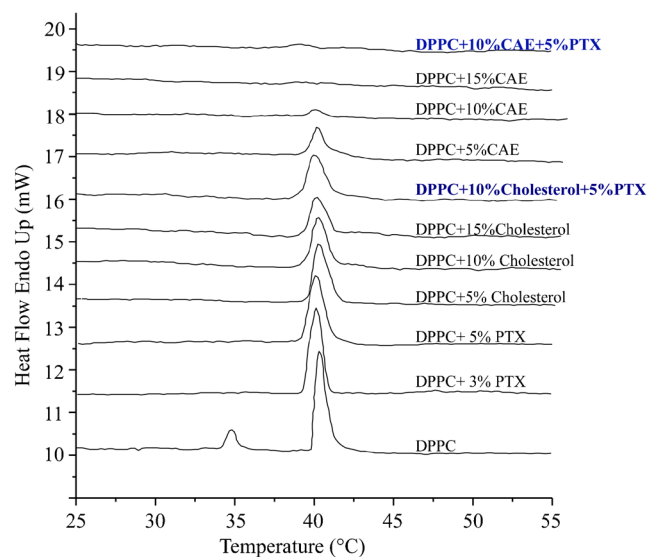


**Fig. 6** Differential Scanning Calorimetry: The DSC thermograms of DPPC liposomes consisting of different concentrations of cholesterol, PTX and CAE.

**Table II** Differential Scanning Calorimetry Parameters

Sr. No.	Liposome formulation	$T_m$ (°C)	$\Delta T_{1/2}$ (°C)	$\Delta H$ (J/g)
1	DPPC	40.49 ± 0.07	0.76 ± 0.03	12.443 ± 0.97
2	DPPC +3% PTX	40.20 ± 0.09	0.92 ± 0.02	11.336 ± 0.92
3	DPPC +5% PTX	40.05 ± 0.08	1.12 ± 0.02	9.213 ± 0.95
4	DPPC +5% Cholesterol	40.31 ± 0.09	1.08 ± 0.03	11.236 ± 0.93
5	DPPC +10% Cholesterol	40.29 ± 0.12	1.08 ± 0.04	7.709 ± 1.12
6	DPPC +15% Cholesterol	40.15 ± 0.14	1.12 ± 0.02	6.062 ± 0.97
7	DPPC +10% Cholesterol +5% PTX	40.00 ± 0.13	1.28 ± 0.04	7.536 ± 1.11
8	DPPC +5% CAE	40.33 ± 0.10	1.08 ± 0.03	4.556 ± 0.94
9	DPPC +10% CAE	40.29 ± 0.14	0.58 ± 0.01	0.832 ± 0.91
10	DPPC +15% CAE	–	–	–
11	DPPC +10% CAE + 5%PTX	–	–	–

for Egg PC and  $-20^{\circ}\text{C}$  to  $-30^{\circ}\text{C}$  for Soya PC). Additionally, the peak corresponding to  $T_g$  is well defined only after prolonged storage of the liposomes below  $T_g$ . Nevertheless, the peak obtained is not as sharp as natural lecithins consisting of mixture of fatty acids. Synthetic lipids on the other hand consist of pure component and thus give sharp peak at their respective  $T_g$  (48,49). Thus, DPPC was selected due to its suitability of studying thermal behavior ( $T_g \sim 41^{\circ}\text{C}$ ) and because it belongs to choline family of phospholipids.

The interactions of PTX and/or cholesterol with DPPC membrane has been widely studied in the past (43,50–52). The addition of PTX or cholesterol is known to abolish  $T_p$  in the DPPC membrane.  $T_p$  is highly sensitive to the presence of other molecules in the polar head region of phospholipids and can not be ascribed to any specific molecular changes. With increasing concentration, PTX shifts the  $T_m$  towards slightly lower temperature with broadening of the main transition with no significant changes in  $\Delta H$ . The broadening of

main transition can be described by  $\Delta T_{1/2}$  which is a measure of the phospholipid assemblies indicating a decrease in size of the cooperative unit. PTX induced changes in  $T_m$  indicates that paclitaxel should be located in outer hydrophobic region of the membrane (43,50,51,53). Cholesterol slightly reduced the  $T_m$  with broadening of the transition peak but markedly reduced the  $\Delta H$  with increasing cholesterol concentration. Cholesterol is assumed to disrupt the ordered array of hydrocarbon chains in gel phase and thereby increasing the fluidity at low concentration and at high concentration, modulating its rigidity by restricting the movement of hydrocarbon chains above  $T_m$  which results in elimination of pretransition and broadening of  $T_g$  (48,52,54,55).

We have studied thermal properties of DPPC liposomes containing different concentration of PTX and cholesterol (Fig. 6 and Table II). As shown in Fig. 6, pure liposomes consisting of only DPPC showed endothermic peak at  $35^{\circ}\text{C}$  corresponding to pretransition ( $T_p$ ) and at  $40.49^{\circ}\text{C}$  corresponding to the main transition ( $T_m$ ). Addition of PTX slightly lowered the  $T_m$  and  $\Delta H$  with broadening of the main transition evident from increase in  $\Delta T_{1/2}$ . This indicates that PTX destabilizes the phospholipid assembly with reduction in cooperativity of the main transition leading to more flexible membrane. Further, the changes in  $T_m$  indicates PTX should be located in outer hydrophobic co-operative zone of the membrane (51). Addition of cholesterol produced very slight reduction in  $T_m$ . Conversely,

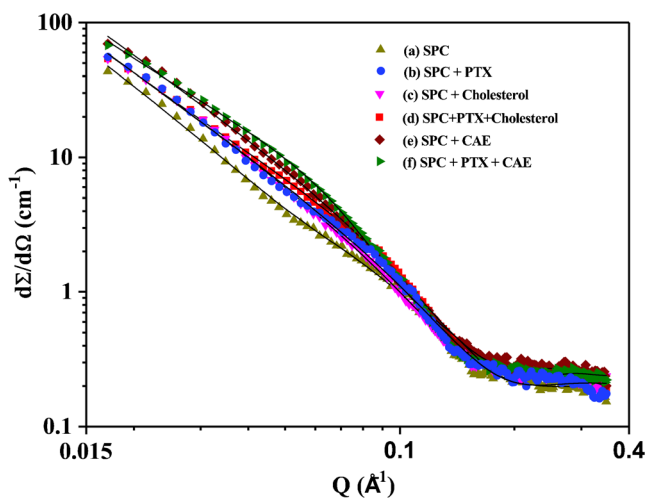


**Fig. 7** Small Angle Neutron Scattering Study: (a) SPC liposomes (b) SPC:PTX (97:3) liposomes (c) SPC:Cholesterol (95:5) liposomes (d) SPC:Cholesterol:PTX (92:5:3) liposomes (e) SPC:CAE (85:15) liposomes and (f) SPC:CAE:PTX (77.5:15:5) liposomes.

**Table III** Bilayer Thickness Determined by SANS

Sr. No.	Liposome composition	Bilayer thickness $t$ (Å)
1	SPC	24.3
2	SPC:PTX (97:3 M ratio)	27.2
3	SPC:Cholesterol (95:5 M ratio)	27.1
4	SPC:Cholesterol:PTX (92:5:3 M ratio)	28.2
5	SPC:CAE (85:15 M ratio)	29.9
6	SPC:CAE:PTX (77.5:15:5 M ratio)	30.1

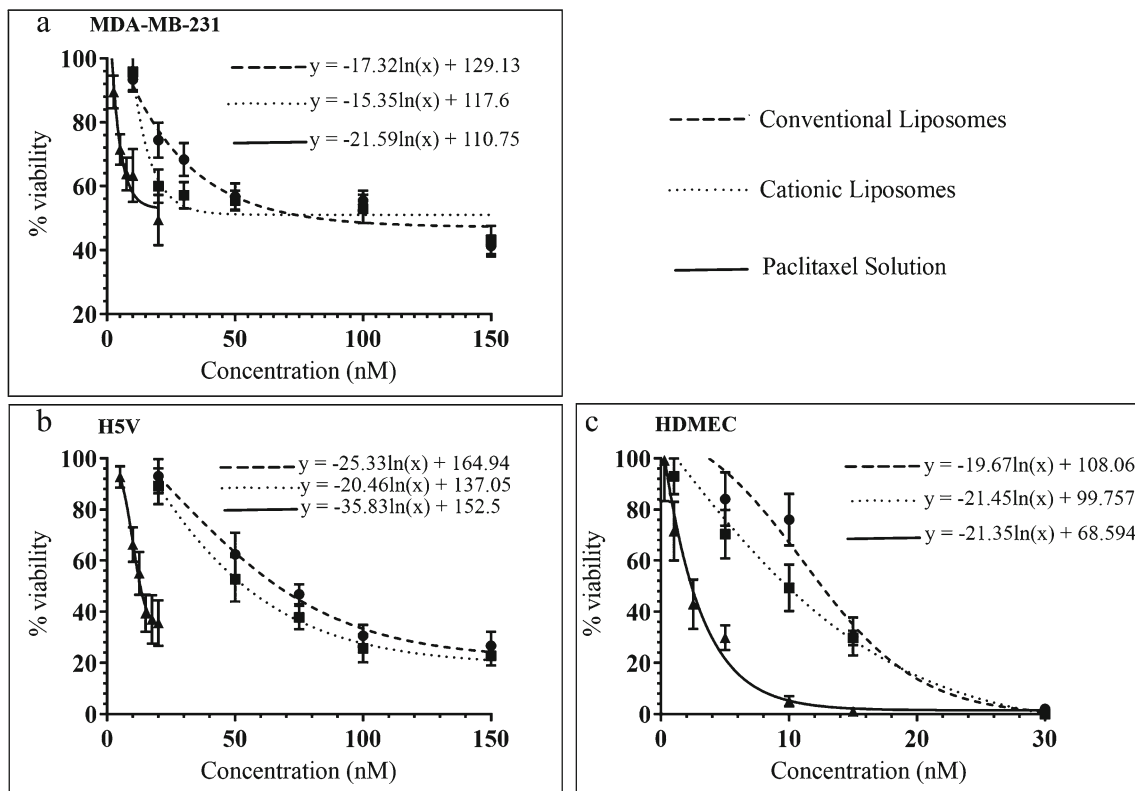


**Fig. 8** Cytotoxicity of PTX solution, conventional liposomes and cationic liposomes after 72 h on (a) MDA-MB 231 cells, (b) H5V cells (c) HDMEC cells. The lines represent non-linear curve fits for each sample. The error bars represent the mean  $\pm$  SD of each value ( $n = 3$ ).

the  $\Delta H$  decreased markedly with slight increase in  $\Delta T_{1/2}$  (Table II). The changes in  $\Delta H$  of main transition depends upon the localization of the molecule within the hydrophobic interior of the membrane rather than the vicinity of the polar head group. In ternary system containing PTX, Cholesterol and DPPC,  $\Delta H$  was reduced significantly compared to DPPC liposomes indicating perturbation of PTX and cholesterol within the hydrophobic core of the membrane.

Addition of CAE in the DPPC liposomes produced pronounced decrease in  $\Delta H$  compared to similar concentrations of cholesterol (Table II) indicating deeper penetration of CAE molecule within the DPPC bilayer. At 15 mol% the main transition and hence enthalpy of transition were completely eliminated. At 10 mol% concentration the  $\Delta H$  was only 0.8 J/g which was not detectable after addition of PTX. This implies that PTX and CAE should be located deeper in the DPPC bilayer which is consistent with the findings of MD simulation.

### Small Angle Neutron Scattering (SANS)

Small Angle Neutron Scattering study was performed to evaluate the vesicular structure and bilayer thickness of the liposomes. Figure 7 shows scattering profiles of liposomes made of different compositions of SPC, PTX, cholesterol and CAE. The liposomes were prepared in the deuterated water as it provides a good contrast between the liposomes and the dispersion medium. The scattering intensity in the low- $Q$  region of the data decreases in a straight line with a slope of  $(-2)$  [as  $1/Q^2$ ], thus indicating the formation of vesicles in these systems. As shown in the Fig. 7, the scattering curves showed typical scattering profiles exhibited by a vesicular system (56). Further the absence of Bragg peaks which occur in the SANS spectra because of multilamellarity in the vesicle was absent in all formulations which confirmed the formation of small unilamellar vesicles.

**Table IV** IC50 value of PTX Formulations on Different Cell Lines

Formulation	MDA-MB 231 cell line	H5V cell line	HDMEC cell line
Conventional liposomes	96.41 nM	93.47 nM	19.13 nM
Cationic liposome	81.76 nM	70.43 nM	10.17 nM
PTX solution	16.67 nM	17.47 nM	2.3 nM

These vesicles have been characterized by the bilayer thickness as the measurement of the size of vesicles is limited by the  $Q_{\min}$  of the SANS instrument. The bilayer thickness obtained from SANS results are given in Table III. In single component bilayer, the hydrocarbon chains of the phospholipids are highly interdigitated above  $T_g$  (57). The  $T_g$  of SPC is well below the room temperature at which SANS was carried out and hence, it was expected that the hydrocarbon chains should be in interdigitated phase and the thickness of the bilayer should be minimum amongst all the measured samples. The SANS data showed that SPC liposomes had lowest bilayer thickness amongst all the samples. The effect of cholesterol on the bilayer thickness has been studied extensively. It is reported that cholesterol increases bilayer thickness by increasing lipid acyl chains ordering in egg lecithin and bilayers consisting of several saturated lipids (58,59). As shown in Table III, the bilayer thickness increased after addition of cholesterol and it is believed to be due to reduction in allowed conformations of the hydrocarbon chain at liquid crystalline state (59). Inclusion of PTX in liposomes increased the bilayer thickness to similar extent. This can be attributed to the area condensing effect similar to that of cholesterol (53). CAE has a similar but more pronounced effect on the membrane thickness. The molecular size of CAE is larger than cholesterol and hence the observed effect of CAE on membrane thickness is more significant than that of cholesterol. We assume that when CAE is incorporated in the bilayer membrane, it extends the bilayer across its hydrophobic chain region thereby making more space for accommodation of PTX molecules within hydrophobic pockets in between the bilayer membrane. This accommodation of PTX along with the size of CAE has a pronounced effect on the membrane thickness as compared to cholesterol containing liposomes which could be possible reason behind higher drug loading and stability of CAE containing PTX liposomes.

### In-Vitro Cytotoxicity Study

The cytotoxicity of PTX in solution was compared with PTX in conventional liposomes and cationic liposomes on three different cell lines, MDA-MB 231, H5V and HDMEC cells. Figure 8 shows % viability of the cell populations at different concentrations. Table IV summarizes IC<sub>50</sub> value of PTX solution and PTX liposomes at 72 h incubation. The IC<sub>50</sub> value for the solution and the liposomes was comparatively higher in MDA-MB 231 and H5V cells than HDMEC cells, most likely because they are transformed cells, whereas the HDMECs are a primary cell line. The PTX solution was more potent (showing lower IC<sub>50</sub> values) as compared to the liposomes in all cell lines. This might be attributed to the slower release of PTX from the liposomal formulation (17). Cationic liposomes showed slightly lower IC<sub>50</sub> values compared to the values for conventional liposomes in all cell lines. Though the difference in conventional liposomes and cationic

liposomes in terms of IC<sub>50</sub> value is small, cationic liposomes may nevertheless provide higher clinical benefits compared to conventional liposomes due to their preferential distribution to the endothelial cells.

### Endothelial Cell Migration Assay

The potential of PTX formulations to inhibit migration of endothelial cells was determined using the Trans-well migration assay. Figure 9 shows the comparison of different PTX formulations and blank liposomes with the control. The control group consisted of cells without any treatment and the blank liposomes group consisted of the liposomes without PTX. Statistical analysis was performed using GraphPad Prism 7.02 software by one-way ANOVA. The blank liposomes showed no effect on migration ability of the endothelial cells. PTX solution at 0.1 nM concentration did not show any significant inhibition ( $p = 0.0985$ ) while at 1 nM concentration it showed very significant inhibition ( $p = 0.0001$ ). On the other hand, conventional liposomes and cationic liposomes showed significant inhibition at 0.1 nM concentration having  $p$ -value 0.0142 and 0.0094, respectively. At higher concentration, i.e. 1 nM, both the formulation showed highly significant inhibition of migration ( $p = 0.0001$ ).

The endothelial cell migration assay was performed at well below the cytotoxic concentration of each formulation. The liposomal vehicles did not show any significant migration

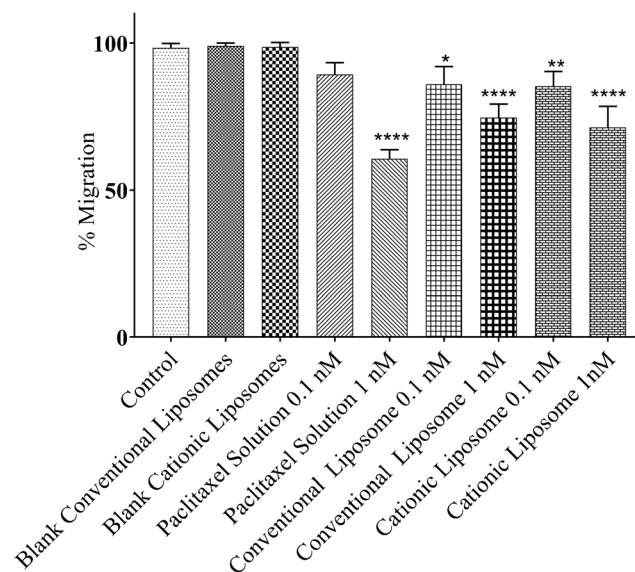


**Fig. 9** Trans-well Migration Assay: After six hours of incubation with test samples, the %migration of treated HDMEC cells was calculated in relation to the untreated (control) HDMEC cells. Blank liposomes (without PTX) did not inhibit the migration of cells. At 0.1 nM PTX concentration, the liposomes and the solution inhibited the cell migration to similar extent. At 1 nM PTX concentration, the solution had slightly higher inhibition potential compared to the liposomes. There was no significant difference in % migration between the solution and the liposomes or between the liposomes. The error bars represent the mean  $\pm$  SD of each value ( $n = 3$ ). (\* represents  $p < 0.05$ , \*\* represents  $p < 0.01$ , \*\*\*\* represents  $p < 0.0001$ ).

inhibition even at the higher concentration used, which indicates that the migration inhibition obtained with PTX encapsulated liposomes was due to the drug only. The liposomal formulation showed significant inhibition at the lower concentration used, which was unexpected, as PTX solution did not show significant inhibition at this concentration compared to the control. However, when analyzed using one-way ANOVA, there was no significant difference between PTX solution and liposome formulation at low concentration. All the formulations could significantly inhibit the migration of endothelial cells at the higher concentration used, which was not cytotoxic to the cells. These results suggest that PTX encapsulated in liposomes maintained efficacy as an inhibitor of endothelial migration.

### Alkaline Comet Assay

The Alkaline Comet assay was performed to determine whether there was any genotoxicity of the synthesized

compound cholesteryl arginine ethyl ester (CAE) and so to establish its safety for pharmaceutical applications. HDMEC and MDA-MB 231 cells were exposed to two levels of CAE; with 5  $\mu\text{g}/\text{ml}$  corresponding to the amount needed to deliver 175  $\text{mg}/\text{m}^2$  dose of PTX and with 50  $\mu\text{g}/\text{ml}$  corresponding to ten times the amount needed for drug delivery (60). The treated cells were compared with control untreated cells. Hydrogen peroxide (200 nM) treatment for 20 min was used as a positive control. Figure 10 (a to h) show representative images of HDMEC and MDA MB-231 cell nuclei stained using SYBR® Gold dye after electrophoresis to separate intact DNA from damaged fragments. The positive control showed the migration of broken strands of DNA forming a tail appearing like a comet (Fig. 10b, f). The negative control group showed cells with a circular appearance (Fig. 10a, e). None of the treatments showed the formation of a tail and the cells appeared circular, like untreated control cells (Fig. 10c, d, g, h).

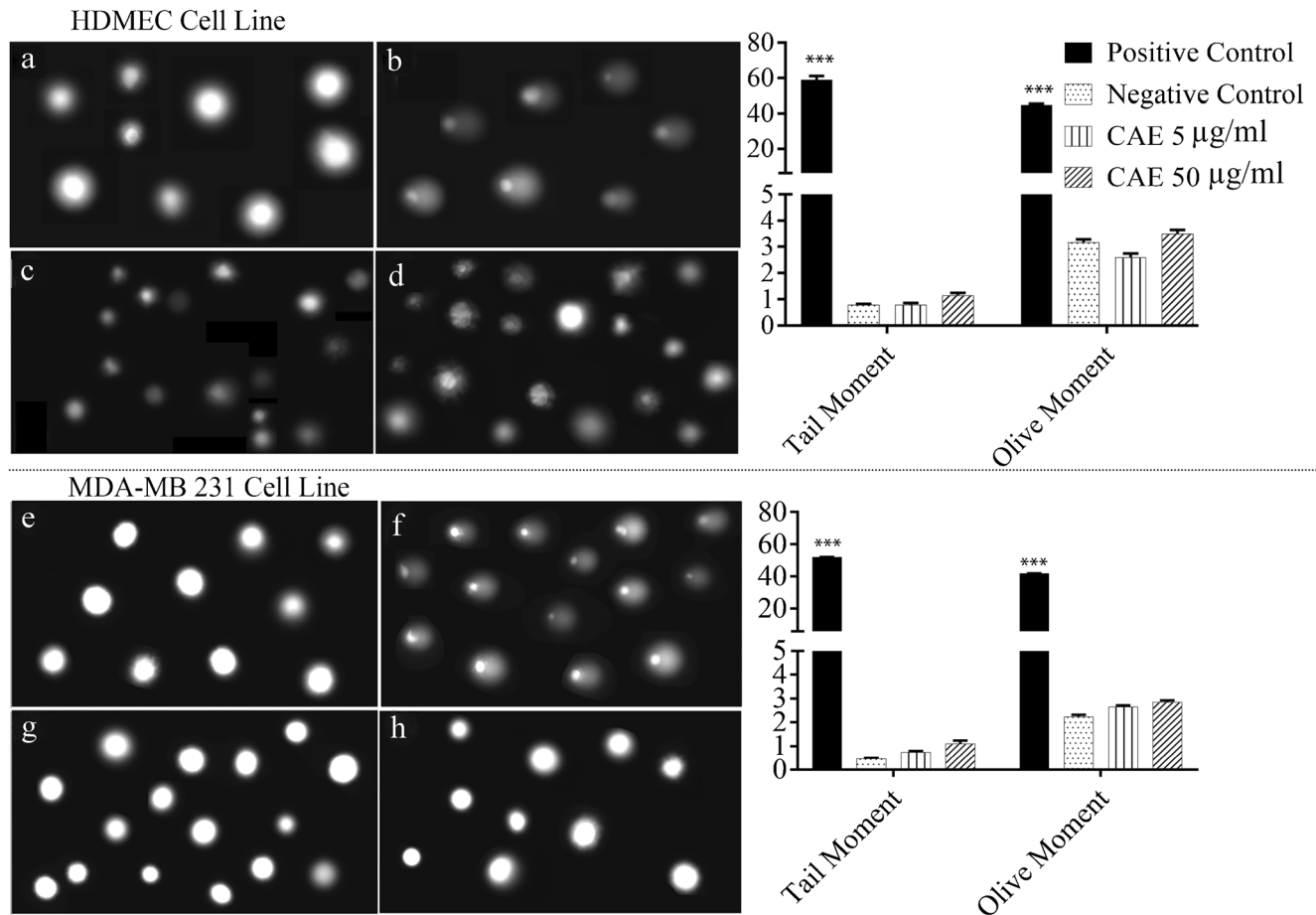


**Fig. 10** Comet Assay and Comet Score: Fluorescence Microscopy Image (20X objective) of HDMEC cells [(a) Negative Control (Untreated) (b) Positive Control (treated with 1 ml, 200  $\mu\text{M}$  H<sub>2</sub>O<sub>2</sub> for 20 min (c) CAE (5  $\mu\text{g}/\text{ml}$ ) treated cells (d) CAE (50  $\mu\text{g}/\text{ml}$ ) treated cells] and MDA-MB231 cells [(e) Negative Control (Untreated) (f) Positive Control (treated with 1 ml, 200  $\mu\text{M}$  H<sub>2</sub>O<sub>2</sub> for 20 min (g) CAE (5  $\mu\text{g}/\text{ml}$ ) treated cells (h) CAE (50  $\mu\text{g}/\text{ml}$ ) treated cells]. Comet score: In HDMEC and MDA-MB231 cells CAE did not cause any significant differences in tail moment and olive moment compared to the untreated (negative control) cells at 5  $\mu\text{g}/\text{ml}$  or 50  $\mu\text{g}/\text{ml}$  concentration of CAE. The 5  $\mu\text{g}/\text{ml}$  concentration of CAE corresponds to the amount needed to deliver a clinical dose PTX in cationic liposomes. The 50  $\mu\text{g}/\text{ml}$  concentration was also tested to ensure safety of CAE. The data are expressed as mean  $\pm$  SD (n = 3). The triple asterisks indicate  $p < 0.001$ .

The results were analyzed using one-way ANOVA with GraphPad Prism 7.02 software. As shown in Fig. 10, both concentrations of CAE tested (5 µg/ml, 50 µg/ml) did not cause any significant difference in the tail moment or olive moment in either HDMEC or MDA-MB 231 cells. This initial analysis by the comet assay indicated that the synthesized compound does not have any genotoxicity. With the help of other techniques, exhaustive safety profile can be generated for establishing the use of the compound in pharmaceutical applications.

## CONCLUSION

It can be concluded that CAE can be used as a membrane stabilizing lipid for the preparation of PTX loaded cationic liposomes. The MD simulation of CAE and PTX incorporated liposomes revealed the possibility of hydrogen bonding between PTX and CAE. In addition to hydrogen bonding, PTX could penetrate deeper in the liposome bilayer, when CAE was used. These factors might be responsible for increased loading and stability of PTX within the bilayer. The DSC results showed that inclusion of CAE in the liposome membrane eliminated  $T_g$  with increasing concentration which could result in increased rigidity of the membrane and hence improved stability. The SANS study showed that inclusion of CAE has a similar effect on the increase in thickness of the liposome membrane as compared to cholesterol. However, the effect is more pronounced than cholesterol suggesting difference in the location and alignment within the membrane. In addition to stability, CAE also provides positive charge to the liposomes in all biological conditions due to guanidinium groups and thus may provide a further advantage over tertiary or quaternary ammonium group containing lipids. The cationic liposomes prepared with CAE and PTX have slightly improved cytotoxicity and ability to inhibit endothelial migration compared to conventional liposomes. The metabolism of CAE should result in formation of cholesterol and arginine through breakdown of carbamate bond and both the component should follow normal metabolic pathways in a biological system. Thus, CAE can be considered as a biocompatible cationic ligand. The absence of genotoxicity supports this hypothesis. The in-vitro results presented here are encouraging and supportive of using CAE as a cationic ligand. Further in-vivo studies are now needed to establish potential utility of CAE in pharmaceutical preparations.

## ACKNOWLEDGMENTS AND DISCLOSURES

The authors are extremely thankful to The British Council, UK and Department of Biotechnology, India for providing a fellowship under the Newton-Bhabha Ph.D. placement program 2015–16 for Mr. Jasmin Monpara, which facilitated the

in-vitro cell studies. Authors are thankful to University Grant Commission (UGC), Government of India, for financial assistance and AICTE-NAFETIC for providing facilities to perform the experimental work. The authors are thankful to Dr. V. K. Aswal and Dr. Debes Ray at the Bhabha Atomic Research Centre, Mumbai, India for help with carrying out the Small Angle Neutron Scattering Study. The authors are thankful to Dr. Spencer Collis and Ms. Caroline Daye, the department of Oncology and Metabolism, The Medical School, The University of Sheffield for help with carrying out the Comet Assay. Authors declare no conflict of interest.

## REFERENCES

1. Surapaneni MS, Das SK, Das NG. Designing paclitaxel drug delivery systems aimed at improved patient outcomes: current status and challenges. *ISRN pharmacology*. 2012;2012:1–15.
2. Singla AK, Garg A, Aggarwal D. Paclitaxel and its formulations. *Int J Pharm*. 2002;235(1–2):179–92.
3. Gelderblom H, Verweij J, Nooter K, Sparreboom A, Cremophor EL. The drawbacks and advantages of vehicle selection for drug formulation. *Eur J Cancer*. 2001;37(13):1590–8.
4. US Food and Drug Administration. Drugs@FDA: FDA approved drug products. 2017. Available from: <https://www.accessdata.fda.gov/scripts/cder/daf.html>.
5. Rizvi NA, Riely GJ, Azzoli CG, Miller VA, Ng KK, Fiore J, et al. Phase I/II trial of weekly intravenous 130-nm albumin-bound paclitaxel as initial chemotherapy in patients with stage IV non-small-cell lung cancer. *J Clin Oncol*. 2008;26(4):639–43.
6. Ruttala HB, Ko YT. Liposome encapsulated albumin-paclitaxel nanoparticle for enhanced antitumor efficacy. *Pharm Res*. 2015;32(3):1002–16.
7. Bernabeu E, Helguera G, Legaspi MJ, Gonzalez L, Hocht C, Taira C, et al. Paclitaxel-loaded PCL-TPGS nanoparticles: *in vitro* and *in vivo* performance compared with Abraxane®. *Colloids Surf B: Biointerfaces*. 2014;113:43–50.
8. Yoshizawa Y, Kono Y, K-i O, Kimura T, Higaki K. PEG liposomalization of paclitaxel improved its *in vivo* disposition and anti-tumor efficacy. *Int J Pharm*. 2011;412(1–2):132–41.
9. Koudelka Š, Liposomal TJ. Paclitaxel formulations. *J Control Release*. 2012;163(3):322–34.
10. Slingerland M, Guchelaar HJ, Rosing H, Scheulen ME, van Warmerdam LJ, Beijnen JH, et al. Bioequivalence of liposome-entrapped paclitaxel easy-to-use (LEP-ETU) formulation and paclitaxel in polyethoxylated castor oil: a randomized, two-period crossover study in patients with advanced cancer. *Clin Ther*. 2013;35(12):1946–54.
11. [clinicaltrials.gov](https://clinicaltrials.gov). A trial evaluating the efficacy and safety of EndoTAG®-1 in combination with paclitaxel and gemcitabine compared with paclitaxel and gemcitabine as first-line therapy in patients with visceral metastatic triple-negative breast cancer. <https://clinicaltrials.gov/ct2/show/NCT03002103>, 2016.
12. Campbell RB, Fukumura D, Brown EB, Mazzola LM, Izumi Y, Jain RK, et al. Charge determines the distribution of liposomes between the vascular and extravascular compartments of tumors. *Cancer Res*. 2002;62(23):6831–6.
13. Lila ASA, Ishida T, Kiwada H. Targeting anticancer drugs to tumor vasculature using cationic liposomes. *Pharm Res*. 2010;27(7):1171–83.

14. Thurston G, McLean JW, Rizen M, Baluk P, Haskell A, Murphy TJ, et al. Liposomes target angiogenic endothelial cells in tumors and chronic inflammation in mice. *J Clin Invest*. 1998;101(7):1401–13.
15. Schmitt-Sody M, Strieth S, Krasnici S, Sauer B, Schulze B, Teifel M, et al. Targeting therapy: paclitaxel encapsulated in cationic liposomes improves antitumoral efficacy. *Clin Cancer Res*. 2003;9(6):2335–41.
16. Bocci G, Di Paolo A, Danesi R. The pharmacological bases of the antiangiogenic activity of paclitaxel. *Angiogenesis*. 2013;16(3):481–92.
17. Yang T, Cui F-D, Choi M-K, Cho J-W, Chung S-J, Shim C-K, et al. Enhanced solubility and stability of PEGylated liposomal paclitaxel: *in vitro* and *in vivo* evaluation. *Int J Pharm*. 2007;338(1–2):317–26.
18. Sofias AM, Dunne M, Storm G, Allen C. The battle of “Nano” paclitaxel. *Adv Drug Deliv Rev*. 2017;122:20–30.
19. Huynh L, Grant J, Leroux J-C, Delmas P, Allen C. Predicting the solubility of the anti-cancer agent docetaxel in small molecule excipients using computational methods. *Pharm Res*. 2008;25(1):147–57.
20. Xiang T-X, Anderson BD. Liposomal drug transport: a molecular perspective from molecular dynamics simulations in lipid bilayers. *Adv Drug Deliv Rev*. 2006;58(12–13):1357–78.
21. Stepniewski M, Pasenkiewicz-Gierula M, Róg T, Danne R, Orłowski A, Karttunen M, et al. Study of PEGylated lipid layers as a model for PEGylated liposome surfaces: molecular dynamics simulation and Langmuir monolayer studies. *Langmuir*. 2011;27(12):7788–98.
22. Kang M, Loverde SM. Molecular simulation of the concentration-dependent interaction of hydrophobic drugs with model cellular membranes. *J Phys Chem B*. 2014;118(41):11965–72.
23. Jämbeck JP, Eriksson ES, Laaksonen A, Lyubartsev AP, Eriksson LA. Molecular dynamics studies of liposomes as carriers for photosensitizing drugs: development, validation, and simulations with a coarse-grained model. *J Chem Theory Comput*. 2013;10(1):5–13.
24. Hristova K, Wimley WC. A look at arginine in membranes. *J Membr Biol*. 2011;239(1–2):49–56.
25. Wang Z. Schotten-Baumann Reaction. In: *Comprehensive Organic Name Reactions and Reagents*. John Wiley & Sons, Inc.; 2010. p. 2536–2539.
26. Gao X, Huang L. A novel cationic liposome reagent for efficient transfection of mammalian cells. *Biochem Biophys Res Commun*. 1991;179(1):280–5.
27. Garlanda C, Parravicini C, Sironi M, De Rossi M, De Calmanovici RW, Carozzi F, et al. Progressive growth in immunodeficient mice and host cell recruitment by mouse endothelial cells transformed by polyoma middle-sized T antigen: implications for the pathogenesis of opportunistic vascular tumors. *Proc Natl Acad Sci*. 1994;91(15):7291–5.
28. Zhang JA, Anyarambhatla G, Ma L, Ugwu S, Xuan T, Sardone T, et al. Development and characterization of a novel Cremophor® EL free liposome-based paclitaxel (LEP-ETU) formulation. *Eur J Pharm Biopharm*. 2005;59(1):177–87.
29. Chen D-B, T-z Y, Lu W-L, ZHANG Q. *In vitro* and *in vivo* study of two types of long-circulating solid lipid nanoparticles containing paclitaxel. *Chem Pharm Bull*. 2001;49(11):1444–7.
30. Aswal V, Small-angle GP. Neutron scattering diffractometer at Dhruva reactor. *Curr Sci*. 2000;79(7):947–53.
31. Hayter J, Penfold J. Determination of micelle structure and charge by neutron small-angle scattering. *Colloid Polym Sci*. 1983;261(12):1022–30.
32. Kaler E. Small-angle scattering from colloidal dispersions. *J Appl Crystallogr*. 1988;21(6):729–36.
33. Chen S-H, Lin T-L. 16. Colloidal solutions. In: Price DL, Sköld K, editors. *Methods in experimental physics*: Elsevier; 1987. p. 489–543.
34. Pedersen JS. Analysis of small-angle scattering data from colloids and polymer solutions: modeling and least-squares fitting. *Adv Colloid Interf Sci*. 1997;70:171–210.
335. Pedersen JS, Riekel C. Resolution function and flux at the sample for small-angle X-ray scattering calculated in position–angle–wavelength space. *J Appl Crystallogr*. 1991;24(5):893–909.
36. Bevington PR, Robinson DK, Blair JM, Mallinckrodt AJ, McKay S. Data reduction and error analysis for the physical sciences. *Comput Phys*. 1993;7(4):415–6.
37. Valster A, Tran NL, Nakada M, Berens ME, Chan AY, Symons M. Cell migration and invasion assays. *Methods*. 2005;37(2):208–15.
38. Lovelock J, Bishop M. Prevention of freezing damage to living cells by dimethyl sulphoxide. *Nature*. 1959;183(4672):1394–5.
39. Instruments P. <http://www.perceptive.co.uk/products/comet-assay-iv/>.
40. Li Y-C, Rissanen S, Stepniewski M, Cramariuc O, Róg T, Mirza S, et al. Study of interaction between PEG carrier and three relevant drug molecules: piroxicam, paclitaxel, and hematoporphyrin. *J Phys Chem B*. 2012;116(24):7334–41.
41. Vander Velde DG, Georg GI, Grunewald GL, Gunn CW, Mitscher LA. "hydrophobic collapse" of taxol and Taxotere solution conformations in mixtures of water and organic solvent. *J Am Chem Soc*. 1993;115(24):11650–1.
42. Stanton DT, Mattioni BE, Knittel JJ, Jurs PC. Development and use of hydrophobic surface area (hsa) descriptors for computer-assisted quantitative structure–activity and structure–property relationship studies. *J Chem Inf Comput Sci*. 2004;44(3):1010–23.
43. Balasubramanian SV, Straubinger RM. Taxol-lipid interactions: taxol-dependent effects on the physical properties of model membranes. *Biochemistry*. 1994;33(30):8941–7.
44. Belsito S, Bartucci R, Sportelli L. Paclitaxel interaction with phospholipid bilayers: high-sensitivity differential scanning calorimetric study. *Thermochim Acta*. 2005;427(1–2):175–80.
45. Lian T, Ho RJ. Trends and developments in liposome drug delivery systems. *J Pharm Sci*. 2001;90(6):667–80.
46. Zhao L, Feng S-S. Effects of cholesterol component on molecular interactions between paclitaxel and phospholipid within the lipid monolayer at the air–water interface. *J Colloid Interface Sci*. 2006;300(1):314–26.
47. Demetzos C. Differential scanning calorimetry (DSC): a tool to study the thermal behavior of lipid bilayers and liposomal stability. *Journal of liposome research*. 2008;18(3):159–73.
48. Ladbroke B, Chapman D. Thermal analysis of lipids, proteins and biological membranes a review and summary of some recent studies. *Chem Phys Lipids*. 1969;3(4):304–56.
49. Taylor KM, Morris RM. Thermal analysis of phase transition behaviour in liposomes. *Thermochim Acta*. 1995;248:289–301.
50. Bernsdorff C, Reszka R, Winter R. Interaction of the anticancer agent Taxol™(paclitaxel) with phospholipid bilayers. *J Biomed Mater Res*. 1999;46(2):141–9.
51. Zhao L, Feng S-S, Kocherginsky N, Kostetski I. DSC and EPR investigations on effects of cholesterol component on molecular interactions between paclitaxel and phospholipid within lipid bilayer membrane. *Int J Pharm*. 2007;338(1–2):258–66.
52. McMullen TP, McElhaney RN. New aspects of the interaction of cholesterol with dipalmitoylphosphatidylcholine bilayers as revealed by high-sensitivity differential scanning calorimetry. *Biochimica et Biophysica Acta (BBA)-Biomembranes*. 1995;1234(1):90–8.
53. Zhao L, Feng S-S. Effects of lipid chain length on molecular interactions between paclitaxel and phospholipid within model biomembranes. *J Colloid Interface Sci*. 2004;274(1):55–68.

54. Ladbrooke B, Williams RM, Chapman D. Studies on lecithin-cholesterol-water interactions by differential scanning calorimetry and X-ray diffraction. *Biochimica et Biophysica Acta (BBA)-Biomembranes*. 1968;150(3):333–40.
55. Estep T, Mountcastle D, Biltonen R, Thompson T. Studies on the anomalous thermotropic behavior of aqueous dispersions of dipalmitoylphosphatidylcholine-cholesterol mixtures. *Biochemistry*. 1978;17(10):1984–9.
56. Yue B, Huang C-Y, Nieh M-P, Glinka CJ, Katsaras J. Highly stable phospholipid unilamellar vesicles from spontaneous vesiculation: a DLS and SANS study. *J Phys Chem B*. 2005;109(1):609–16.
57. Braganza LF, Worcester DL. Hydrostatic pressure induces hydrocarbon chain interdigitation in single-component phospholipid bilayers. *Biochemistry*. 1986;25(9):2591–6.
58. Levine Y, Wilkins M. Structure of oriented lipid bilayers. *Nature New Biology*. 1971;230(11):69–72.
59. McIntosh TJ. The effect of cholesterol on the structure of phosphatidylcholine bilayers. *Biochimica et Biophysica Acta (BBA)-Biomembranes*. 1978;513(1):43–58.
60. Squibb B-M. Taxol®(paclitaxel) injection package insert. 2000. In: 2008. US Food and Drug Administration. *Drugs@ FDA: FDA approved drug products*. 2017. Available from: <https://www.accessdata.fda.gov/scripts/cder/daf/index.cfm?event=overview.process&ApplNo=020262.html>.